

[1963]

18 p ref

[REDACTED]

NATIONAL AERONAUTICS AND SPACE ADMINISTRATION.
Lewis Research Center, Cleveland, Ohio

[REDACTED] *

LEWIS TECHNICAL PREPRINT 5-63

[REDACTED]

no N64 14263* Lewis TP-5-63

CODE-1
(NASA TMX-51,129) OTS:

HEAT-TRANSFER ASPECTS OF SPACE RADIATORS

OTS PRICE

		<u>1.60 ph.</u>
XEROX	\$	
		<u>1.80</u>
MICROFILM	\$	



By Seymour Lieblein

[Signature]

[REDACTED]

Presented at AICHE/ASME
6th
Prepared for the Sixth National Heat Transfer Conference
Sponsored by the American Institute of Chemical
Engineers and The American Society
of Mechanical Engineers, Boston, Mass.
Boston, Massachusetts August 11-14, 1963

HEAT-TRANSFER ASPECTS OF SPACE RADIATORS \

By Seymour Lieblein

National Aeronautics and Space Administration
Lewis Research Center
Cleveland, Ohio

ABSTRACT

141263 ~~10164~~

Thermal radiators are required for closed-cycle space powerplants to dissipate cycle waste heat. The basic problem is to provide for the removal of this heat in compact lightweight components of high reliability. Space power cycles requiring waste-heat radiators are discussed, and heat removal systems and radiator characteristics are described.

The basic heat-transfer paths from working fluid to radiator outer surface are traced and recent developments in these areas are presented. First, internal fluid heat-transfer coefficients in liquid-metal- and gas-filled tubes are discussed. The second consideration involves the two-dimensional conductive heat transfer through the tube and fin cross section. Finally, for the third path of net emission from the radiator surface, such factors as the effects of tapered fins, various fin-tube geometries, and meteoroid bumpers are considered.

R J T 402

INTRODUCTION

Heat-transfer considerations have always played an important role in the development of terrestrial powerplants. There is no reason to believe that the situation should be different for the case of powerplants intended for use in space. In fact, the nature of the space environment and the required performance levels of spacecraft render heat-transfer considerations a most vital factor in the development of space power-conversion systems.

This paper will discuss some of the heat-transfer factors involved in the design of high-power electric generating systems for advanced space missions. It will examine a component of the powerplant (the heat rejection system), trace the principal heat flow paths involved, and show how heat-transfer theory and knowledge can be used to influence the design and performance of the system.

In format, powerplant characteristics and heat-rejection component configurations and requirements will first be described. Considerations and recent developments dealing with internal-flow heat transfer, conduction through solid portions, and radiation from external surfaces will then be presented. The results contained herein were obtained by members of the Flow Processes Branch of the NASA Lewis Research Center and also by Professor E. M. Sparrow and associates of the University of Minnesota under contract to the NASA.

[REDACTED]

SPACE POWERPLANTS

Powerplants for the production of large amounts of electric power in space will most likely be of either the turbogenerator or thermionic-emitter type. The thermionic-emitter power-conversion system in principle produces electricity directly by the movement of electrons from a hot surface to a cold surface. Turbogenerator power-conversion systems require the use of a working fluid in a heat power cycle. Diagrams of the basic elements of two turbogenerator power cycles are shown in figure 1. The principal components of the Rankine or vapor cycle are revealed in figure 1(a). A nuclear reactor or solar heat source is used to provide heat to boil a fluid such as mercury, potassium, rubidium, etc. The vapor then drives the turbine, which in turn drives the generator to produce the desired electric power output. The turbine vapor exhaust must then be condensed and its heat of condensation removed ultimately by means of thermal radiation to space. The requirement of thermal radiation for the removal of waste heat in the cycle is a unique feature of space powerplants.

A Brayton or gas cycle turbogenerator system can also be used as shown in figure 1(b). In this cycle, a heated inert gas such as argon, neon, etc. is used to drive the turbine and the generator; sensible heat is removed from the gas in the radiator and the cooled gas is then returned to the cycle through a compressor. For increased efficiency a recuperator will most likely be used in a real application (ref. 1). Temperature-entropy diagrams for both cycles are shown on the right of the figure.

The thermionic-emitter power-conversion system will also require a radiator and fluid loop in order to maintain the low temperature of the anode. In this case the radiator, as in the case of the gas cycle, will be a single-phase radiator.

For the Rankine cycle turbogenerator system, there are several ways in which the vapor exhaust from the turbine can be condensed and its heat of condensation rejected to space, as shown in figure 2. A direct condenser is shown in figure 2(a). In this configuration, the vapor from the turbine passes directly into a radiator in which the vapor condenses on the inside of tubes. Its heat of condensation is then radiated to space from the outer surfaces of the tubes (radiation cooled). In the second method, as shown in figure 2(b), a heat exchanger, such as the shell and tube variety, can be used to condense the vapor. The radiator for this case must then supply subcooled liquid to absorb the heat of condensation of the vapor (convection cooled). The radiator working fluid is then a single phase with decreasing temperature from inlet to outlet. In the third method (fig. 2(c)), vapor exhausting from the turbine can be mixed physically with subcooled liquid from the radiator. This concept is called the jet condenser. In this configuration, as before, the radiator is a single-phase type. It is thus seen that space radiators can either be of the two-phase variety, in which fluid temperature is essentially constant along the flow path, or of the single-phase variety, in which a gas or liquid flows at decreasing temperature.

CASE FILE COPY

RADIATOR CHARACTERISTICS

A sketch of a fin-and-tube radiator currently being considered for these powerplants is shown in figure 3. This radiator applies specifically to a direct condenser type but its features are generally characteristic of most types of radiators. Here, vapor from the turbine exhaust enters a header, which distributes the vapor to a large number of parallel tubes. The vapor condenses in these tubes and the condensate is collected in the header at the outlet. The individual tubes are separated by heat-conducting fins, which perform as extended heat-transfer surfaces.

Typical cross sections of the fin-and-tube configurations are shown in the lower part of the figure. On the left, the tube has an internal liner that is resistant to the corrosion effects of liquid-metal working fluids. Around this liner is a sleeve of armor which protects the tube against damaging impact from meteoroids. The fin between the tubes is also shown. The second configuration on the right shows an alternative method of protecting the tube against damage from impacting meteoroids. Instead of using a very thick armor shield, a displaced bumper is used in order to fragment the impacting particles.

Figure 4 shows that the surface area required for waste-heat radiators for high-power systems can be extremely large. Radiator prime (constant temperature) specific area in square feet per kilowatt of power output is plotted against radiator temperature for the three principal types of power-conversion systems. Curves for peak temperatures of 1540° and 2040° F are shown for the Brayton and Rankine turbogenerator cycles and for peak temperatures of 2640° and 3000° F for the thermionic cycle.

The figure indicates that gas cycles required between 30 to 60 square feet per kilowatt of power output; Rankine cycles, between 1 and 2 square feet per kilowatt; and thermionic converters can get as low as 1/2 square foot per kilowatt for the temperature ranges indicated. Thus, for example, a 1-megawatt Rankine cycle turbogenerator system may require between 1000 and 2000 square feet of radiator area.

The powerplant designer is constantly striving to reduce the radiator area because of its marked influence on radiator weight, vulnerability to meteoroid impact, and integration into the vehicle structure. Obviously, heat-transfer considerations are expected to exert a prime influence on the radiator area and weight problem.

HEAT-TRANSFER PATHS

Let us now look at a typical radiator section, trace the various heat flow paths, and identify the heat-transfer problems involved. In figure 5 is shown a schematic of a typical fin-tube radiator configuration. In the center of the tube, a fluid, either gas, liquid, or vapor, flows and re-

leases its heat to the inner surface of the tube. This involves considerations of convection and condensation heat transfer. If a liquid metal fluid is used, the tube may be composed of an inner liner and an armor sleeve. Heat from the fluid must then pass by conduction through the sleeve and the armor. Part of this heat flows to the outer surface of the tube to be radiated, while part of the heat flows into the adjacent fins. This constitutes a two-dimensional conduction flow from tube to fin with possible flow across a metal-to-metal interface.

Heat from the tube flows down the fin, where it is ultimately dissipated to space from the fin surfaces. Since the fin surface temperature may vary considerably, and since the tube surface temperature also may vary somewhat, there is a matter of radiant interchange between tube and tube and between fin and tube as shown by the dashed lines. Radiation from the outer surfaces of the fin-tube configuration is then further complicated by the existence of solar radiation and also radiation and reflections from a nearby planet or adjacent vehicle component.

Thus, three basic heat-flow problems are involved. The first is the internal-fluid heat transfer, either convection or condensation. The second is the conduction through the solid portions of the fin and tube, and third is the radiation from the outer surfaces and the net heat transfer from the tube configurations. Some recent developments and considerations in these three major heat-transfer areas will now be discussed.

INTERNAL HEAT TRANSFER

Information on internal flow heat transfer for liquid metals, such as sodium, potassium, NaK, and mercury, is for the most part quite scarce. Some information exists for convection heat-transfer coefficients for liquid flow (ref. 2), but condensing heat-transfer coefficients for liquid metals are currently quite uncertain. Experiments are now underway at the General Electric Co., and other investigations will be forthcoming on the flowing condensing coefficients of potassium in single tubes. There seems to be a general difficulty, however, in accurately determining experimentally the temperature drop from fluid to tube wall. Investigation of overall heat-transfer coefficients of multitube condensers will commence soon at the NASA Lewis Research Center. It is hoped that improved information on liquid-metal condensing heat-transfer coefficients might be obtained in the next year or two.

A considerably better picture can be obtained of the internal-flow heat-transfer characteristics of gas radiators. Convection heat-transfer coefficients for gas flow are readily calculated, and the effects of these coefficients on radiator characteristics have been established. For example, figure 6 shows the effect of flow Reynolds number in the radiator tubes on radiator specific weight (lb/kw) for several gases in turbulent flow. These results (taken from ref. 3) are for a 100-kilowatt gas cycle using a bare

tube radiator, that is, tubes without any internal fins. The tube diameter was kept constant at 0.5 inch, the pressure drop across the radiator amounted to 0.08 of the inlet pressure, the equivalent sink temperature (ref. 4) was -60°F , and the fluid temperature in the radiator decreased from 455°F at the inlet to 75°F at the outlet. Reynolds number was varied by changing the system operating pressure.

It is clear from the figure that for all three gases it is desirable to achieve as high a heat-transfer coefficient as possible by increasing the Reynolds number. A low heat-transfer coefficient results in a large radiator weight, because the associated large drop in temperature between the fluid and tube results in an increased surface area requirement.

The performance of the rotating machinery is also improved by increasing the Reynolds number if the size is held constant (ref. 5). The attainment of high Reynolds numbers, however, often decreases the size of the rotating machinery sufficiently to seriously impair its performance. High flow Reynolds numbers, therefore, cannot generally be used, especially in low power level systems. Accordingly, the use of bare radiator tubes will result in very low heat-transfer coefficients and correspondingly high radiator specific weights.

In an effort to increase the heat-transfer coefficients of the radiator tubes, internal finning can be used to advantage. Figure 7 shows the effect of internal finning on heat-transfer coefficient. The effective heat-transfer coefficient (based on tube inside circumference) is plotted against the ratio of the fin wetted area to the tube wetted area for the configuration shown on the figure. The variation in the area ratio was obtained by changing the number of fins while the inside tube diameter and core diameter were held constant at 1.5 and 0.658 inches, respectively. In order to maintain a relatively low pressure drop it may be necessary to restrict the flow to the laminar regime. Accordingly, data for figure 7 were taken at a Reynolds number of 300 (ref. 6). The results show that a considerable relative improvement in the heat-transfer coefficient can be obtained by internal finning.

The use of internal finning for gas radiators, of course, does not come without its penalties. Internal finning may result in increased pressure drop and also in increased weight per unit length of the tubes. Depending upon the thickness of the fin, the unit weight increases involved may not be exactly insignificant. The ultimate effectiveness of internal finning, however, must be determined by optimization programs that consider concurrently the effects of heat-transfer coefficient, pressure drop, internal fin weight, and meteoroid protection.

CONDUCTION HEAT TRANSFER

The two-dimensional heat transfer in the cross section of one quadrant of a fin-tube configuration is shown in figure 8. The temperature on the

inner surface of the tube T_i was assumed constant at 1760°R and isotherms were then computed for the tube and the fin as shown in the figure. The calculation considered the radiant interchange between the fin and the tube. A considerable drop in temperature can occur between the inner surfaces of the tube and the base of the fin, depending upon the particular temperatures and geometries of the fin. In this particular case, the temperature drop was almost 70° . In general, the greater the ratio of heat radiated from the fin to that radiated from the tube, the larger will be the temperature drop from the tube to the fin base.

Similar two-dimensional calculations were made for a series of geometries, materials (Al, Be, Mo, Cb-lZr), and temperatures for a 1-megawatt direct radiator system. The exact two-dimensional heat transfer radiated from these configurations was compared with several simplified techniques for computing the net heat transfer. Results of these calculations are shown in figure 9, where two-dimensional heat transfer values are plotted against heat-transfer values obtained by using three different one-dimensional techniques for the same geometry. The data are taken from reference 7. Points indicated by the triangles considered no drop in temperature from the inside of the tube to the outside of the tube, that is, T_i is equal to T_o . It is assumed that the full tube outer area is the tube radiating surface and that there is no interchange between fin and tube. As can be seen on the curve, the calculation produces an exaggerated heat flux. The second method, shown by the circles, computes a radial or one-dimensional temperature drop across the tube wall with interchange and full tube radiating area. This method compares well with the two-dimensional method. It was also interesting to observe that using just the projected area of the tube with no interchange at all (square symbol) produced a heat flux which was fairly close to that of the two-dimensional calculation. However, this correlation may not be true in general.

Two-dimensional conduction theory has also been used to determine the heat-transfer performance of materials with anisotropic properties (ref. 7). An example for a pyrolytic graphite fin is shown in figure 10, where the isotherms of a 0.010-inch-thick radiator fin are plotted for two orientations of the pyrolytic graphite. The ratio of conductivities was taken as 500 for the two directions. In figure 10(a), the poor conductivity direction is parallel to the axis of the tube. In figure 10(b) the poor conductivity is perpendicular to the plane of the fin. Substantial temperature gradients are produced in the cross section of the fin for this orientation. The net heat flux from the pyrolytic graphite fins, however, are fairly high, 3500 and 3320 Btu per hour per foot, respectively, for the two orientations, as compared with only 1900 to 2200 Btu per hour per foot for regular (commercial) graphite fins (thermal conductivity $k = 25$ to 55 Btu per hour per foot per $^\circ\text{F}$) of the same dimensions.

RADIATION HEAT TRANSFER

The net heat transferred from a fin-and-tube radiator, of course, will depend upon the radiation from the surface of the fins and tubes. As indicated previously, this involves radiant interchange between fin and tube and also between any adjacent planets or vehicle components, as well as inputs from solar radiation. Considerable information exists in the literature on computing the net heat transfer from fin-and-tube configurations and the optimization of these configurations into radiator systems (e.g., refs. 4, 8, 9, and 10). Such theory is based on one-dimensional considerations and fins of rectangular cross section.

In an effort to obtain maximum heat rejection per unit weight for a finned-tube radiator, schemes such as tapered fins can be used. Figure 11 shows the results of an analysis that was made to illustrate the effect of tapering of the fin on the net heat transfer per unit weight of the fin-tube combination (ref. 11). In the figure the ratio of maximum heat radiated to radiator weight is plotted as a function of ratio of fin length to tube outer radius. Calculations are made for several fin tapers from the rectangular cross section given by $y_l/y_0 = 1$ to the trapezoidal cross section with $y_l/y_0 = 0.5$ and the triangular form with a ratio of 0. Superimposed on the plots are values of the conductance parameter N_c . Results are given for two tube internal diameters and a fin base temperature of 1700°R .

In general, tapering the fin can result in an increase in the ratio of heat radiated to weight. Calculations for a 1-megawatt powerplant system, as shown in figure 11, as well as for a 30-kilowatt system indicate that the weight saving involved in the use of triangular tapered fins instead of rectangular fins is about 10 percent. This advantage is likely to be reduced, however, when considerations of tube pressure drop and header weight are included in the analysis.

In the preceding discussions, the fin-tube configuration considered was that of a central fin between tubes. Actually, a wide range of other configurations is possible. Some of these are illustrated in figure 12. On the left are shown various fin-tube geometries that can be used in employing the armor principle. On the right are configurations that can be used that embody the bumper principle. With respect to the configurations on the left, one might question whether there are any large differences in the heat-transfer capabilities of these configurations.

An indication of such a comparison is shown in figure 13. Here, the fin-and-tube radiating effectiveness is plotted against the ratio of fin length to tube radius for several configurations, as shown on the figure. These configurations include central fin geometries and open and closed sandwich configurations. The square configurations were used for ease of calculation. The results from references 12 and 13 show that there really is no marked difference in the radiating effectiveness of these different

configurations. The choice of configuration can thus depend primarily on such factors as vehicle configuration, materials, meteoroid protection, and fabrication without serious regard to heat-transfer characteristics.

For the fin-tube configurations involving the bumper concept, it is obvious that some reduction in heat-transfer capability will result because of the separation between the shield and the tube. An approximate indication of the reduction of the heat-transfer capability is indicated in figure 14 for a circumferential bumper with a spacing between the bumper and the tube proper. If, for the moment the effect on the fin is neglected, and the bumper and tube are taken as concentric cylinders, the relative heat-rejection rate can be computed. The relative heat-rejection rate is defined as the amount of heat radiated from the tube itself if the bumper were not present. This ratio has been plotted against the bumper spacing in tube diameters for two values of emittance in figure 14. It is seen that in the practical range of spacing values, between 0 and about 1 diameter, a considerable reduction in tube heat-rejection rate might result from the use of the bumper.

Increased bumper diameter will also have an adverse effect on the radiating effectiveness of the fin between the tubes, as shown in figure 15. Here, fin radiating effectiveness is plotted against the ratio of bumper radius to fin length for several values of design parameter. Again, as the diameter of the bumper increases, the fin effectiveness is reduced. Of course, the true situation is not quite so simple as indicated by these ideal representations. However, these curves do show that heat-transfer impedance will have to be closely examined in the final determination of the effectiveness of the bumper concept in reducing radiator weight and in improving reliability.

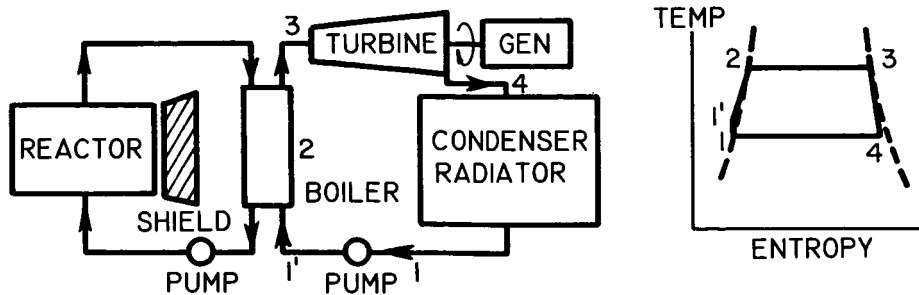
CONCLUSION

Space radiator design can be strongly influenced by heat-transfer considerations such as internal-flow convection and condensation, conduction through solid portions, and net radiation from the outer surfaces. The ultimate success of space radiator development will certainly depend to a large extent on the development of good heat-transfer theory and experimental data.

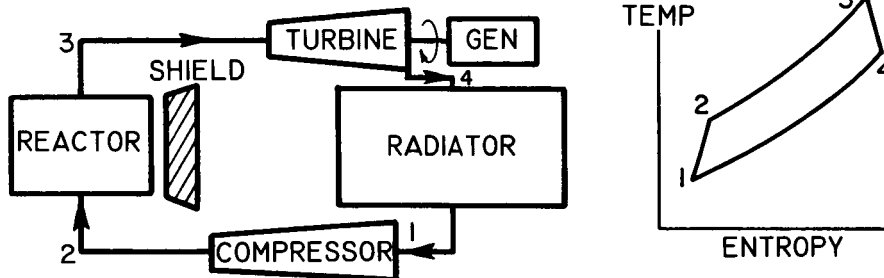
REFERENCES

1. Glassman, Arthur J., Krebs, Richard P., and Fox, Thomas A.: Brayton Cycle Nuclear Space Power Systems and Their Heat Transfer Components. AICHE Preprint No. 57, ASME-AICHE Sixth National Heat Transfer Conference, Boston, Mass., August 11-14, 1963.

2. von Glahn, Uwe H.: Empirical Equation for Turbulent Forced-Convection Heat Transfer for Prandtl Numbers from 0.001 to 1000. NASA TN D-483, 1960.
3. Saule, A. V., and Krebs, Richard P.: Analysis of Sensible Heat Space Radiators. NASA TN to be published.
4. Lieblein, Seymour: Analysis of Temperature Distribution and Radiant Heat Transfer Along a Rectangular Fin of Constant Thickness. NASA TN D-196, 1959.
5. Bullock, R. O.: Analysis of Reynolds Number and Scale Effects on Performance of Turbomachinery. Engineering Report AD-5076-R, Garrett Corp., February 1, 1963.
6. de Lorenzo B., and Anderson, E. D.: Heat Transfer and Pressure Drop of Liquids in Double-Pipe Fin-Tube Exchangers. Trans. ASME, November 1945, pp. 697-702.
7. Stockman, Norbert O., and Bittner, Edward C.: Two-Dimensional Heat Transfer in Fin-Tube Radiators. NASA TN to be published.
8. Sparrow, E. M., and Eckert, E. R. G.: Radiant Interaction Between Fin and Base Surfaces. Jour. Heat Transfer (Trans. ASME), ser. C, vol. 84, no. 1, Feb. 1962, pp. 12-18.
9. Schreiber, L. H., Mitchell, R. P., Gillespie, G. D., and Olcott, T. M.: Techniques for Optimization of a Finned-Tube Radiator. Paper 61-SA-44, ASME, 1961.
10. Haller, Henry C., Krebs, Richard P., and Bittner, E. C.: Analysis and Design Procedures for a Direct Condensing Central Finned Tube Radiator. NASA TN to be published.
11. Haller, Henry C., Lieblein, Seymour, and Auer, B. M.: Heat Rejection and Weight Characteristics of Finned Tube Space Radiators with Tapered Fins. NASA TN to be published.
12. Sparrow, E. M., and Minkowycz, W. J.: Heat-Transfer Characteristics of Several Radiator Finned-Tube Configurations. NASA TN D-1435, 1962.
13. Haller, Henry C.: Comparison of the Heat Rejection and Weight Characteristics of Several Radiator Finned-Tube Configurations. NASA TN to be published.



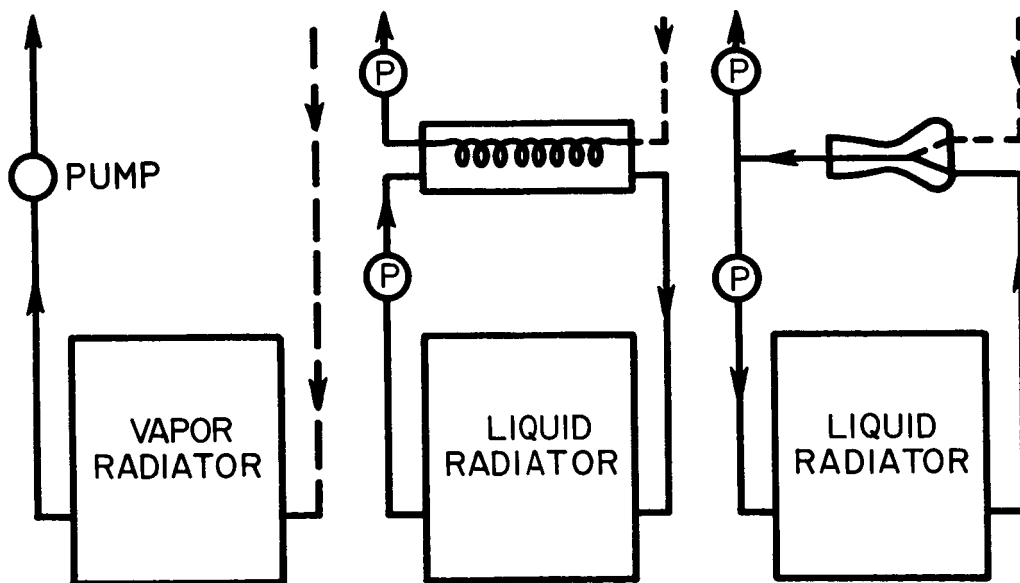
(a) RANKINE (VAPOR) CYCLE.



(b) BRAYTON (GAS) CYCLE.

CS-25586

Figure 1. - Basic elements of turbogenerator power cycles.



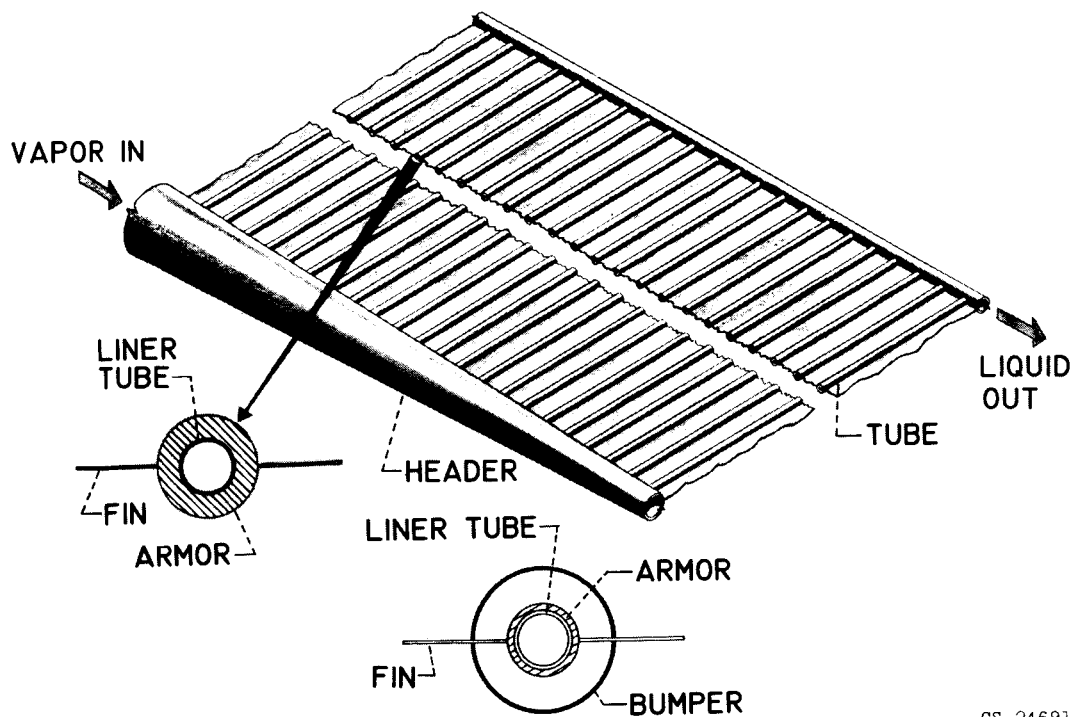
CS-25587

(a) DIRECT CONDENSER.

(b) HEAT-EXCHANGER CONDENSER.

(c) JET CONDENSER.

Figure 2. - Condensing methods for Rankine cycle.



CS-24691

Figure 3. - Fin-and-tube radiator.

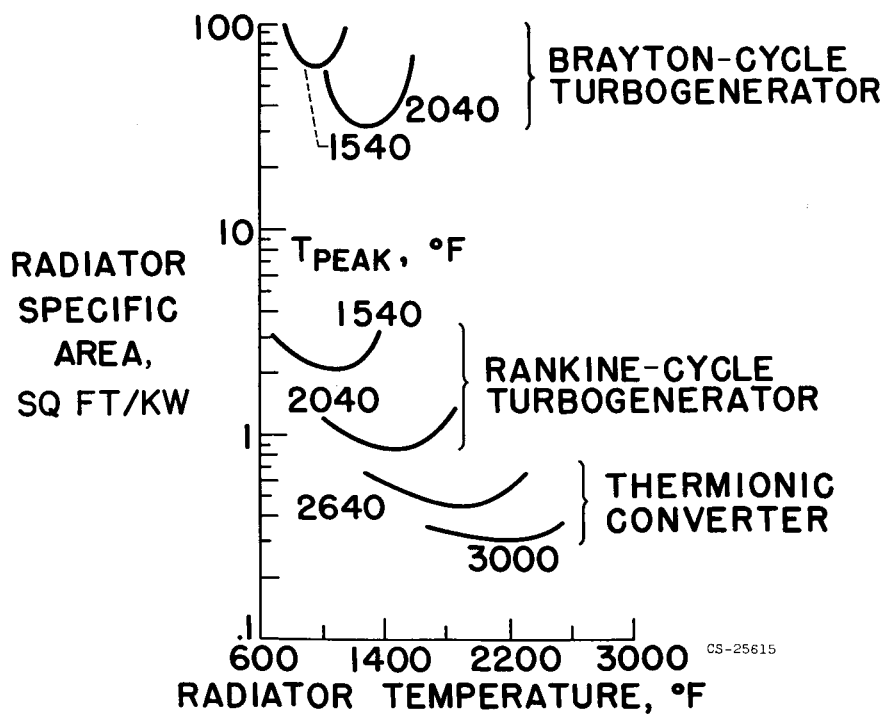
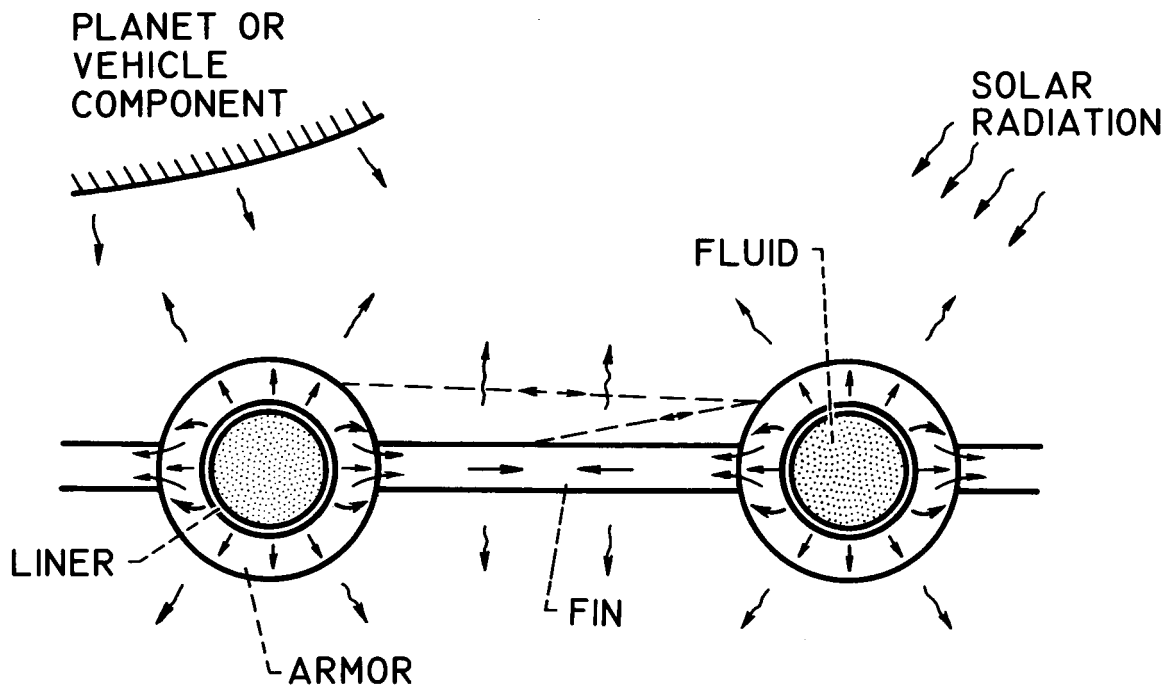
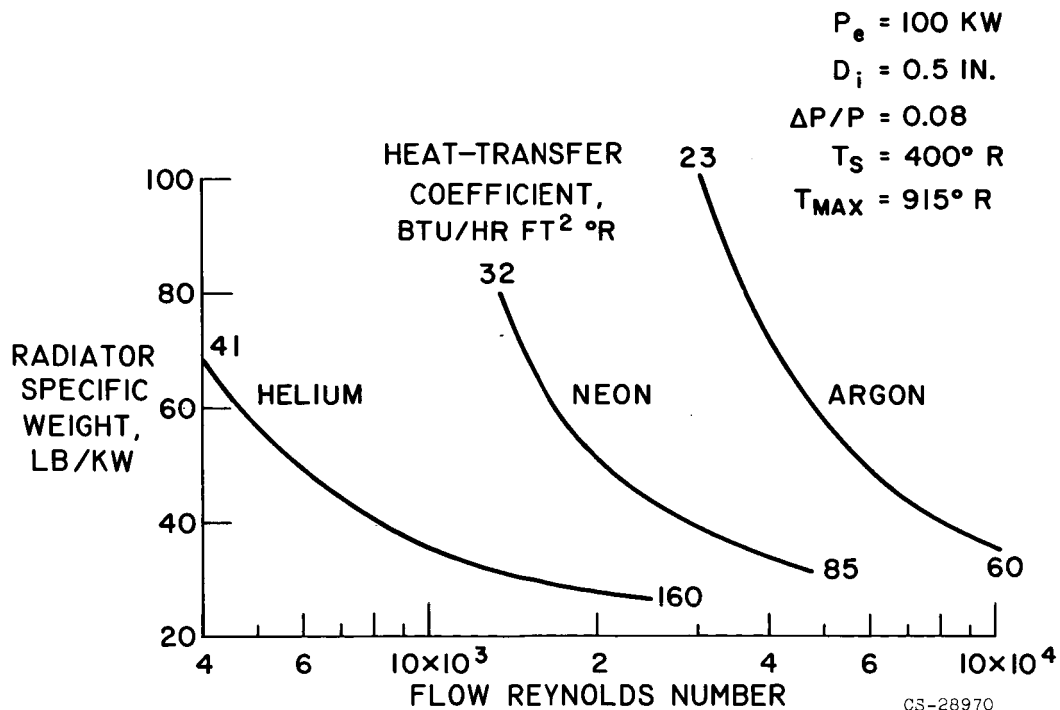


Figure 4. - Radiator-specific-area requirements for several power-conversion systems.



CS-28967

Figure 5. - Radiator heat-transfer paths.



CS-28970

Figure 6. - Effect of flow Reynolds number on Brayton cycle radiator weight for bare tubes.

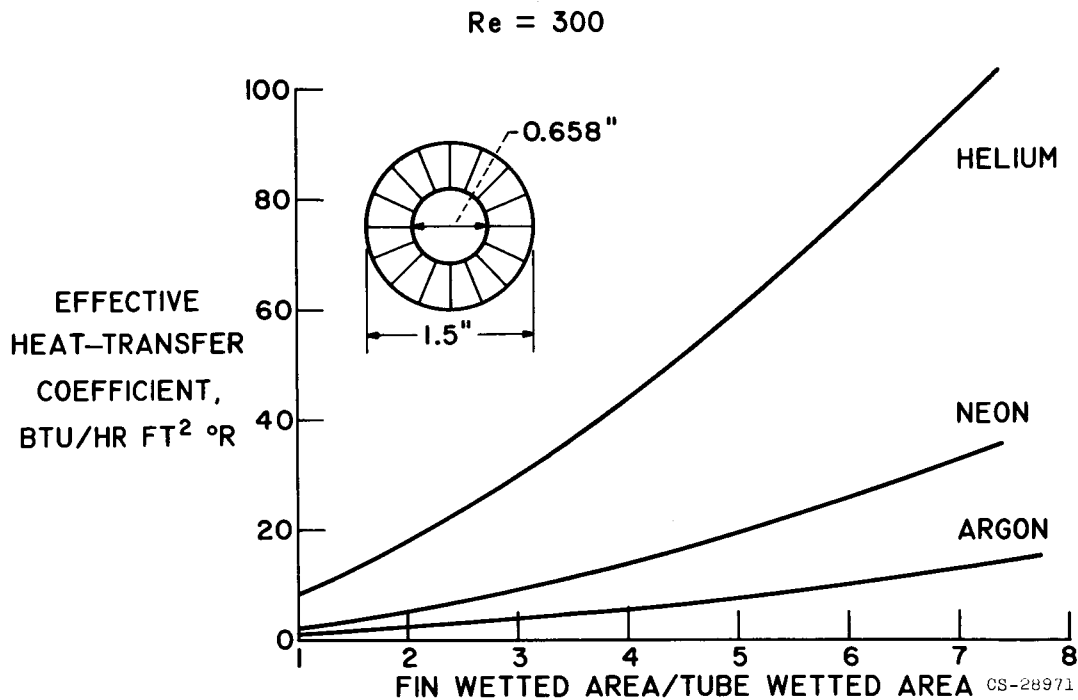


Figure 7. - Effect of internal finning on heat-transfer coefficient for gas flow.

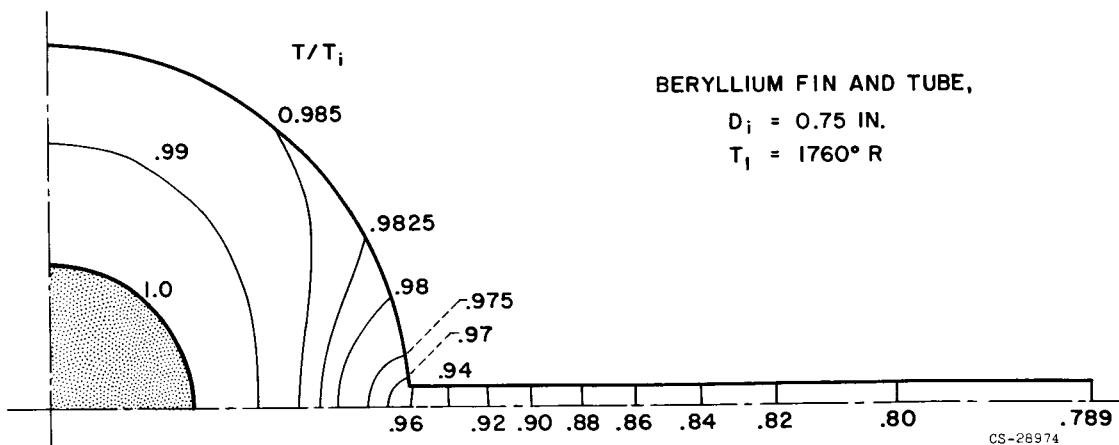


Figure 8. - Isotherms in quadrant of fin-tube configuration.

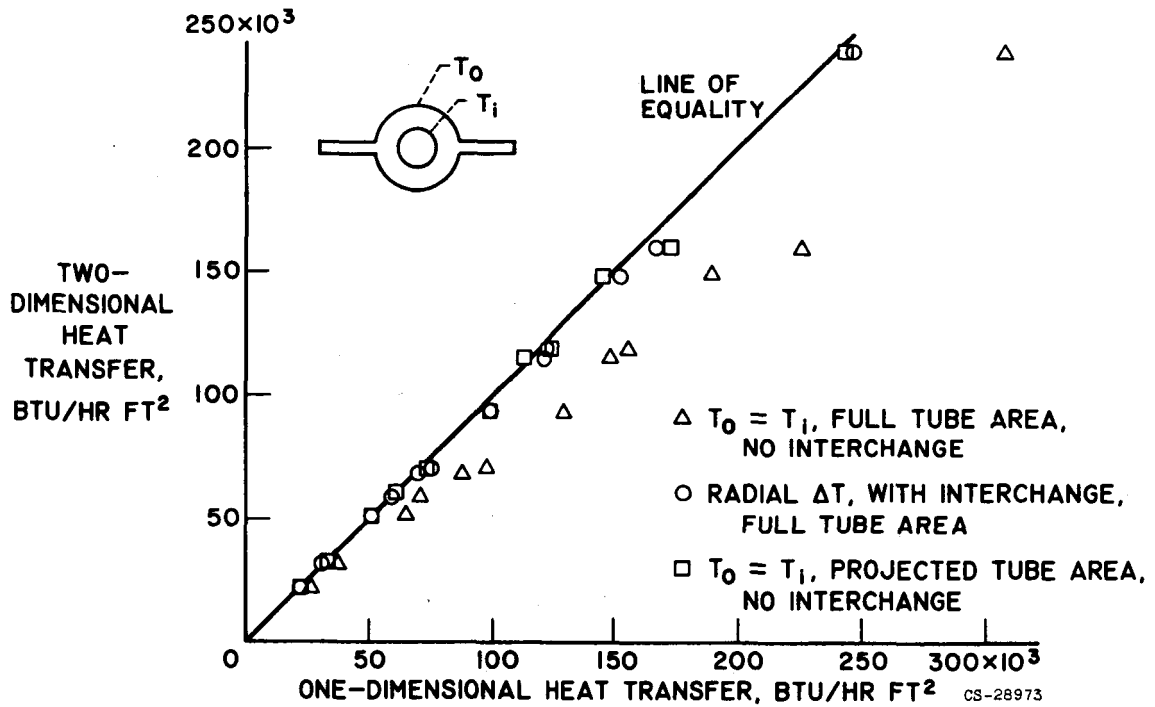


Figure 9. - Comparison of calculation methods for net heat radiated from fin-tube configurations.

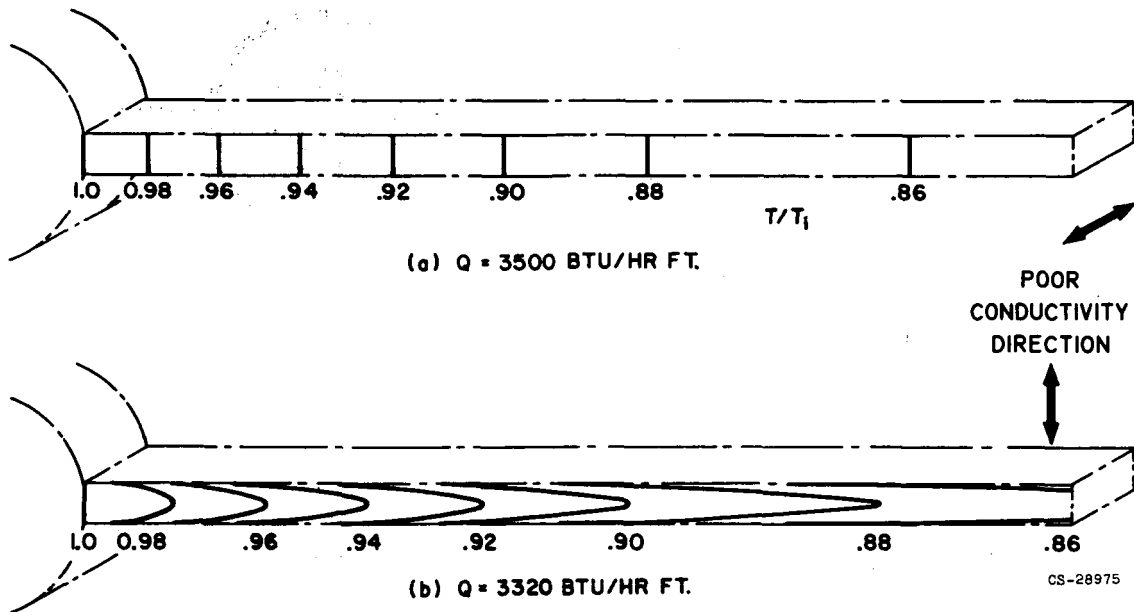


Figure 10. - Isotherms for pyrolytic graphite fins. T_1 , 1350° F.

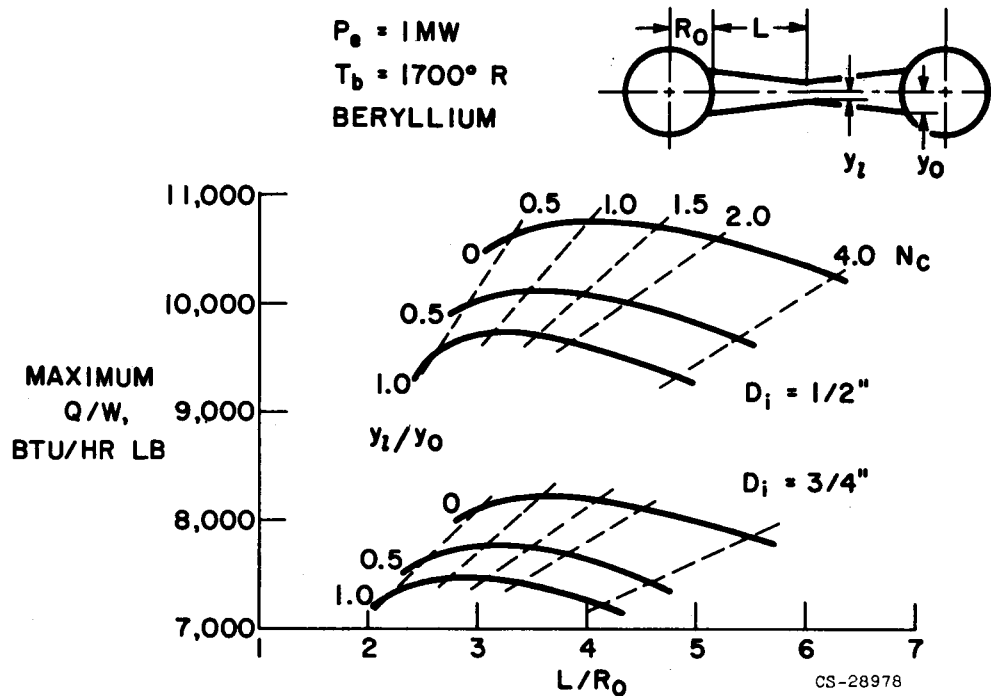


Figure 11. - Effect of fin taper on fin-tube ratio of heat radiated to weight.

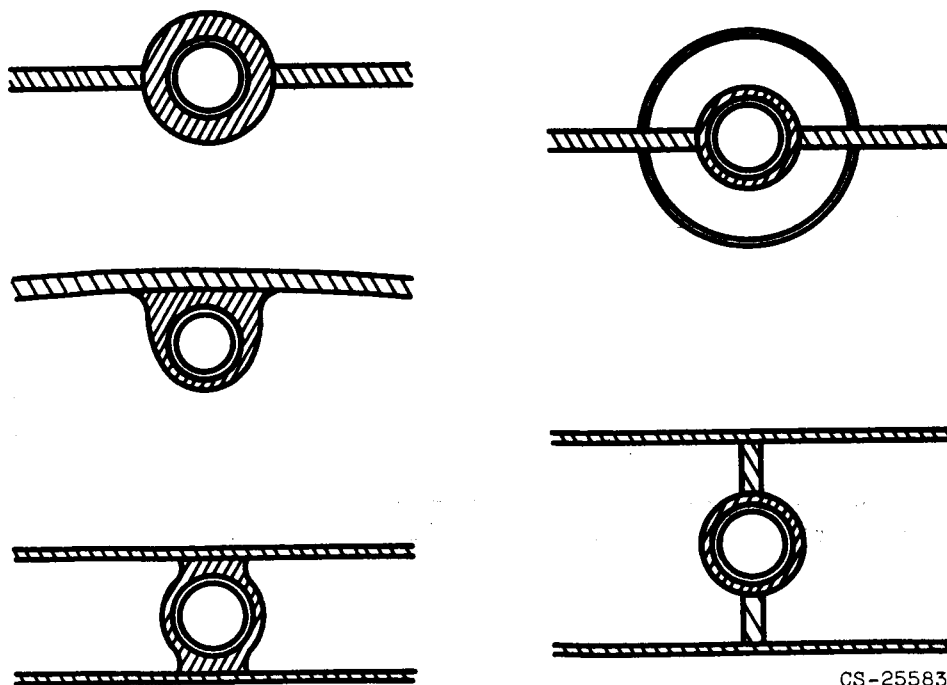


Figure 12. - Fin-and-tube geometries.

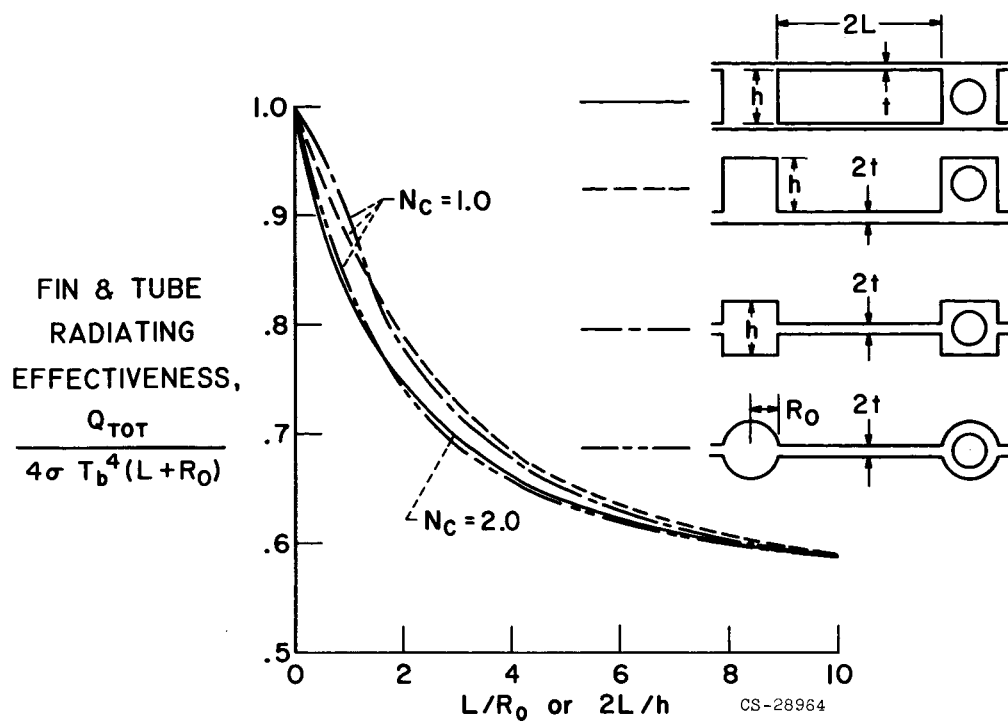


Figure 13. - Comparison of fin-and-tube configurations.

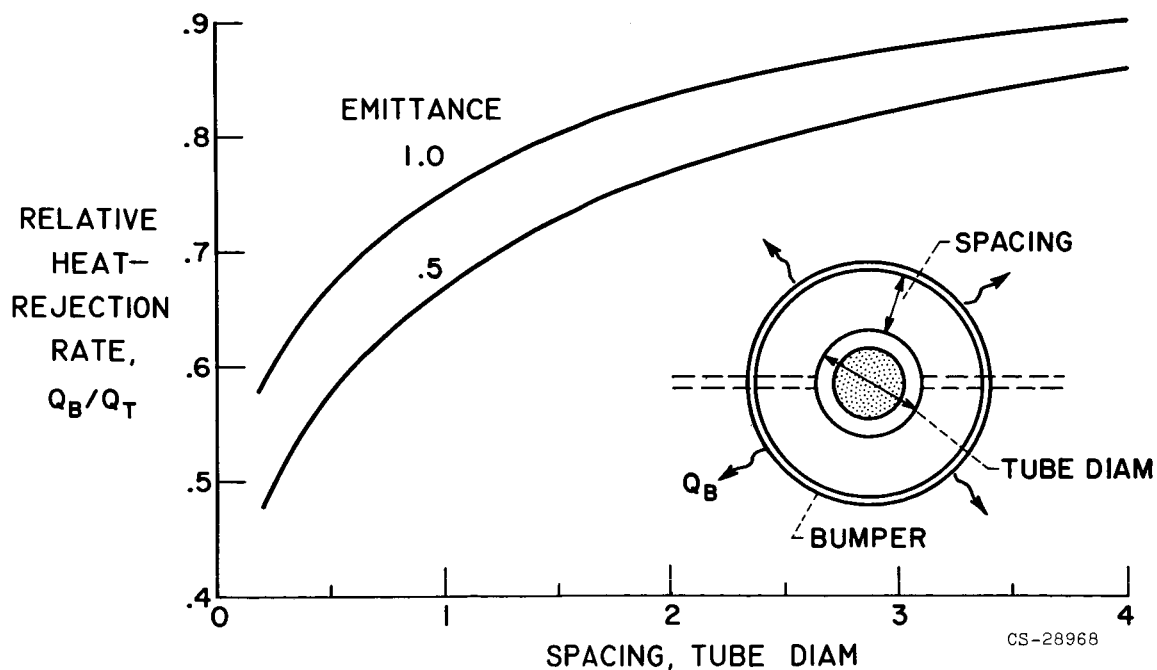


Figure 14. - Effect of meteoroid bumper on tube heat-rejection rate.

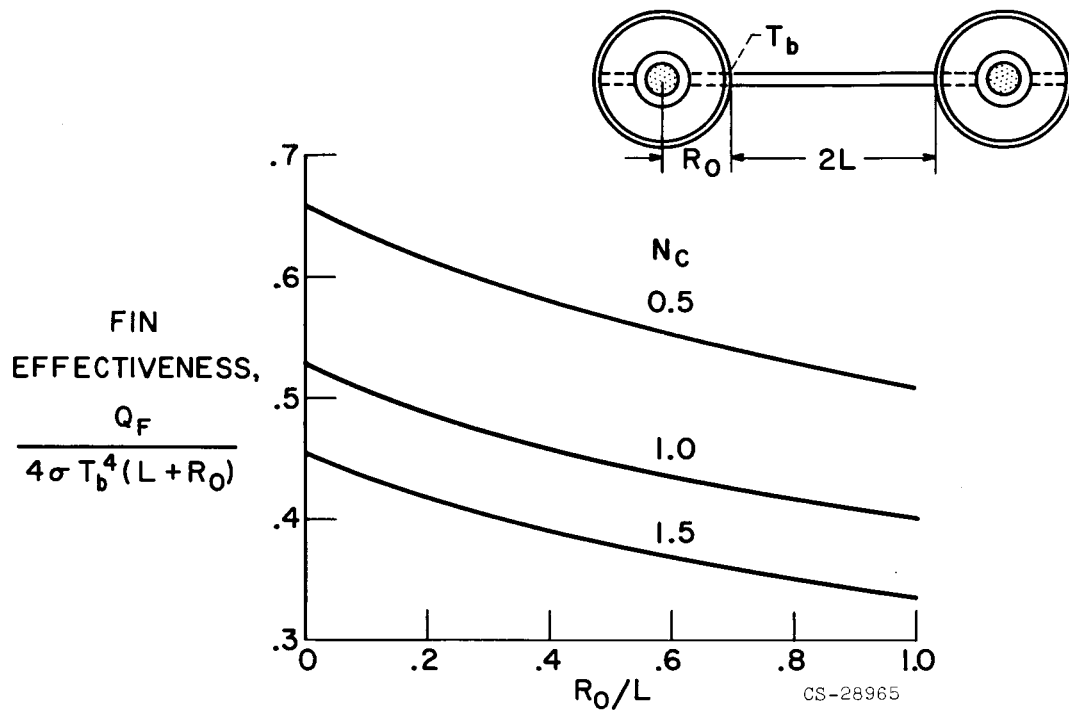


Figure 15. - Effect of meteoroid bumper on fin radiating effectiveness.